高速并行双光子激光直写光刻系统

王洪庆[1]，温积森[1]，杨臻垚[1]，汤孟博[1]，孙秋媛[1]，马程鹏[1]，王子昂[2]，詹兰馨[1]，张晓依[1]，曹春[1]，
沈小明[1]，丁晨良[1*]，匡翠方[1,2**]

[1]之江实验室智能芯片与器件研究中心，浙江 杭州 310023；
[2]浙江大学光电科学与工程学院现代光学仪器国家重点实验室，浙江 杭州 310027

摘要 双光子激光直写技术以其高精度、高灵活性的特点在科研领域被广泛应用，但较低的直写速度制约了其在工业领域的应用与发展。本团队基于转镜扫描系统设计并验证了一套高速双光子激光直写光刻系统，该系统基于空间光调制器与多通道声光调制器的联合调控，实现了六通道并行刻写功能，且每个通道可独立调控，调控频率可达 MHz 以上。实验结果表明，每通道直写速度最高可达 7.770 m/s，刻写特征尺度最小为 150 nm，并行刻写时的最高直写速度可达 46.62 m/s。此外，本团队基于反射式像旋转器设计了一种高精度调节通道间距的方法，调节精度优于 1 nm。

关键词 光学制造；微纳加工；双光子激光直写；多光束并行制造

中图分类号 O439 **文献标志码** A **DOI**：10.3788/CJL202249.2202009

1 引 言

近几年，双光子三维(3D)激光直写技术获得了飞速发展，逐渐成为一种成熟的微纳加工技术[1-3]。双光子 3D 激光直写利用飞秒激光脉冲引发的双光子聚合效应，可以实现超越衍射极限的超高精度 3D 结构加工，在微纳机电系统[4]、超材料[1]、光子晶体[5-6]、微流控器件[7-8]、微纳光学器件[9-10]、生物医疗[11-12]等领域具有巨大的应用潜力。然而，目前该技术的应用大多还停留在实验室环境中，工业上的应用非常有限。制约这项技术向工业发展的一个主要原因是直写速度较慢。提高直写速度的一个简单有效的方法是使用多光束并行刻写代替单光束刻写。目前，已经有一些利用空间光调制器(SLM)或衍射光学元件(DOE)产生多光束并行刻写的研究报道[1, 13-17]。SLM 可以对光束波前进行像素级调制，调制后的光斑经过物镜后在像平面上形成多个焦点，利用扫描器件就可以实现多光束刻写。在多光束刻写策略中，对于任意一个图形，可以将其分解为多个不同的区域，每个区域分配一束激光进行刻写。在大多数情况下，每个分解区域的形貌是不同的，因此需要独立控制每束光的开关，以实现不同形貌的刻写。但在目前的大多数工作中，多光束刻写的开关是同步的，无法进行独立控制。有研究人员利用 SLM 刷新全息图的方法来实现每束光的独立开关[15,17]，但受限于 SLM 的刷新速度，这种独立控制多光束开关的方式难以真正有效提高直写速度。另外，使用不同的运动扫描器件也是影响直写速度的一个关键因素。在目前的研究中，通过压电位移台来实现运动控制是比较常见的方式[18-21]。然而，压电位移台的扫描速度较慢，仅能实现 0.1～10 mm/s 量级的扫描。一个实现更快扫描速度的办法是使用振镜扫描[22-26]。相较于压电位移台，振镜的惯性小，其速度可提升 1～2 个数量级。近期，有研究人员利用共振式振镜实现了更高速的扫描，扫描速度最高可达 8 m/s[27]，但加工精度较低，特征尺寸为 1～4 μm。

为了有效提升双光子激光直写的速度，本团队设计并验证了一种基于转镜的多光束并行刻写方法，将独立多光束并行刻写与高速扫描器件整合在一起。对于独立多光束并行刻写，利用 SLM 生成多光束，再通过多通道声光调制器(AOMC)对多光束的每束光进行独立调制。对于高速扫描器件，利用多面体转镜代替传统振镜，再结合高速空气轴承位移台与压电位移台实现高速 3D 扫描。多面体转镜是一种以稳定速度沿一个方向高速旋转的多面体反射镜，它不同于振镜，没有往复运动，可以实现更高的扫描速度和更高的速度稳定性。最终的测试结果表明，本团队所提方法实

现了单通道7.770 m/s的直写速度,最多可实现六通道同步并行刻写,等效于最高速度为46.62 m/s。此外,为了弥补AOMC器件通道间距为固定值的不足,本团队设计了一种像旋转装置,实现了通道间距的连续可调。

2 基本原理(实验仿真)

2.1 多光束产生方法

本团队采用权重GS算法[28]计算产生六光束的全息图。权重GS算法的基本思想与GS算法一致,不同之处是在迭代过程中不断地通过权重修改所期望的目标光场的振幅,加速迭代过程,提高均匀度。利用上述算法思想在MATLAB上进行全息图的制备和仿真。计算产生六通道的光束阵列,可以发现经过38次迭代之后可以得到图1(a)所示的相位全息图;经过聚焦后,在焦平面上的仿真光斑如图1(b)所示;仿真的六通道光束的均匀度U[29]达到了理想的100%,如图1(c)所示。
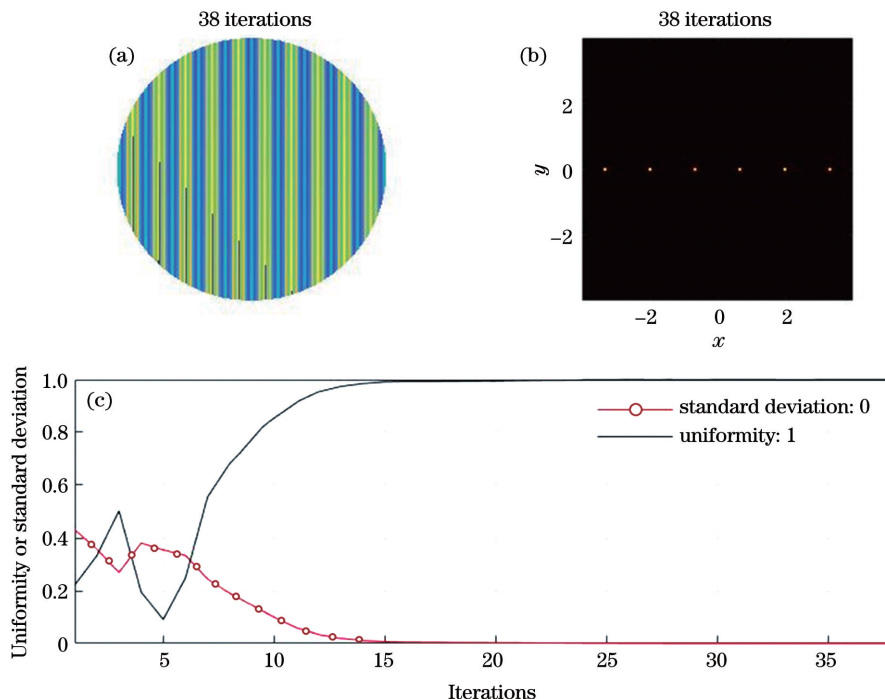

图1 基于权重GS算法进行光束分束的仿真计算结果。(a)六光束阵列的全息图;(b)六光束阵列的聚焦光强;(c)六光束阵列的均匀度与标准差随迭代次数的变化

Fig. 1 Simulation results of beam separation obtained with weighted GS algorithm. (a) Hologram of six-beam array; (b) focused light intensity of six-beam array; (c) variation of six-beam array's uniformity and standard deviation with the number of iterations

2.2 多光束高速独立调控实现方法与系统设计

本团队设计的多光束并行双光子激光直写实验系统如图2所示。图2(a)展示了本系统的3D结构效果图与实物照片(插图),系统整体采用大理石结构设计,配合Bilz EPPC主动隔振系统;大理石为双层结构,下层为激光器、预补偿压缩模块以及样品台模块,上层为多光束调制与扫描光路。图2(b)展示了本系统的光路设计。一台780 nm光纤飞秒激光器(CARMEL CFL-10RFF,平均功率为1 W,重复频率为80 MHz,脉宽为90 fs)用来提供飞秒激光光源。一个光栅对压缩模块包括一片780 nm半波片以及两片透射式衍射光栅,用于预补偿飞秒激光在后续光路中传播时产生的群速度色散[30]。在本系统中,需补偿的群速度色散约为20000 fs²。扩束镜用于将飞秒激光光斑扩束到8 mm。SLM用于产生多光束。入射光的偏振方向须调节到与SLM液晶分子的初始方向一致。本次实验使用一片780 nm半波片调节入射到SLM的偏振,使衍射级能量最大。入射光与反射光之间的夹角小于10°。后续通过第一组4f透镜组对光斑进行缩束,缩束是为了使光束聚焦到AOMC通道时能有更好的相位匹配。第二组4f透镜配合AOMC独立控制每一束光束的开关。该器件包含6个独立的光通道,声光介质为TeO₂,上升沿时间为30 ns,通道孔径大小为0.33 mm×1 mm,通道间距为2.5 mm。第二组4f透镜将SLM处的光斑成像到转镜平面。转镜前放置像旋转器,用于调节多光束排列方向与转镜扫描方向的夹角。关于像旋转器,下文将进一步说明。通过转镜后,光束进入由扫描镜、套筒透镜和物镜(Leica HC-PL-APO-100x/1.40-OIL-STED-WHITE)组成的光学系统。样品台由真空吸附台、压电Z向/偏摆平台、垂直位移台以及XY扫描台组成。照明光源使用LED灯,CMOS相机使用工业相机。
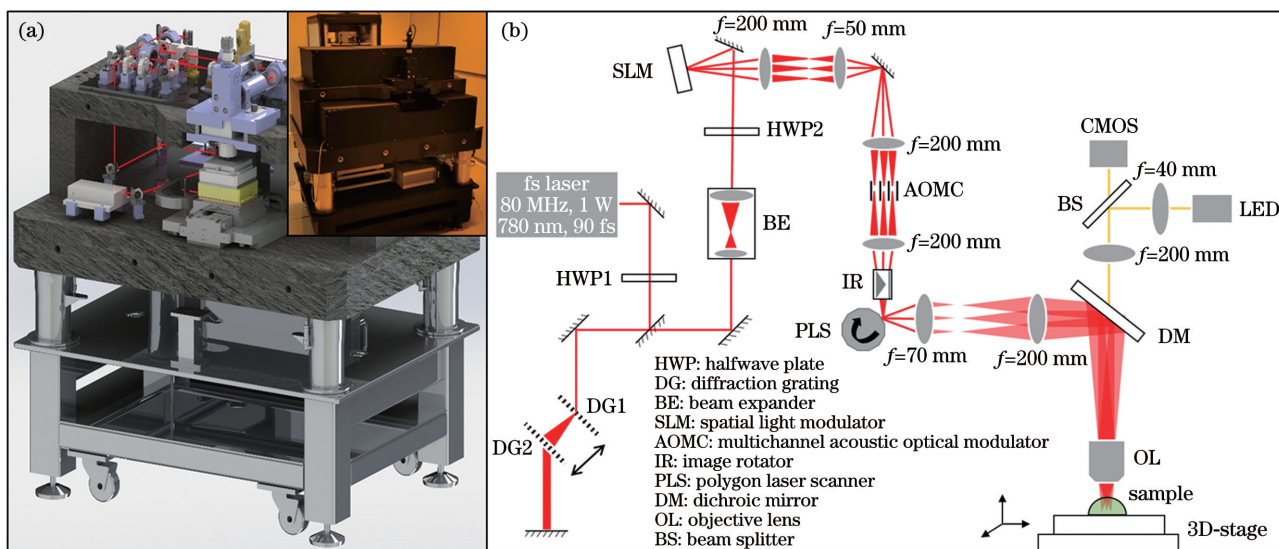
在转镜之前放置像旋转器,可以调节多光束排列方向与转镜扫描方向的夹角,从而实现通道间距连续

图 2　基于转镜扫描的多光束并行双光子激光直写系统。(a)实验装置图；(b)光路图

Fig. 2　Multibeam parallel two-photon laser direct writing system based on polygon laser scanner. (a) Experimental setup; (b) optical path diagram

可调。本团队参考了传统的像旋转器——道威棱镜，并针对本系统进行了优化。道威棱镜是透射式像旋转器，会出现色散与能量损失的问题。为了解决这一问题，可利用棱镜与反射镜设计反射式像旋转器。图 3 是像旋转器的设计与仿真结果。该像旋转器由一面反射镜与一块棱镜组成，棱镜为等腰三角形结构，顶角为 $120°$，腰长为 26 mm。反射镜与棱镜的相对位置满足 $2L_R = L_P$，其中 L_R 表示反射镜到棱镜顶角的距离，L_P 表示棱镜的腰长。采用 Lighttools 软件进行仿真，可以观察三光束情况下的像旋转效果。图 3(a)所示为三个光源，其中边缘两束光源的间距设置为 12.5 mm（这与实际系统中六通道 AOMC 相距最远的两束光的距离相同），夹角为 $3.6°$，光斑大小为 2 mm。像旋转器放置在距离光源 80 mm 处。三光束在传播过程中逐渐重合，重合位置为不动面。在不动面后放置一个焦距为 50 mm 的平凸透镜，用于定性模拟实际系统中由扫描镜、场镜和物镜组成的光学系统的效果。透镜前焦面与不动面重合，后焦面处放置观察面。图 3(b)～(d)是观察面上获得的仿真结果，分别表示像旋转器为 $0°$、$22.5°$ 和 $45°$ 时探测器上的图像。这里定义图 3(a)中像旋转器的状态为 $0°$。可见，透镜焦平面处的图像随着像旋转器的旋转而旋转。与道威棱镜相同，像旋转器与观察面的旋转角度满足两倍关系。图 3(b)～(d)所示的观察面分别旋转了 $0°$、$45°$ 和 $90°$。
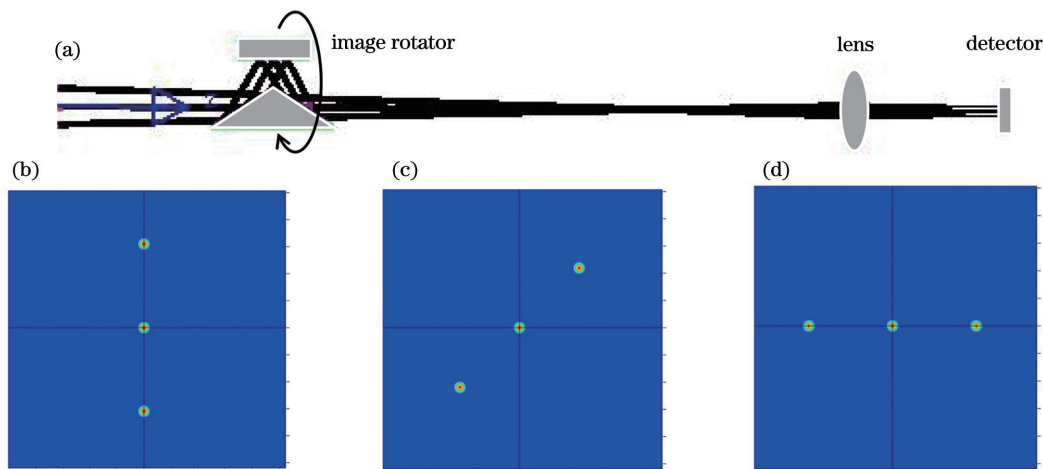

图 3　像旋转器设计方案与仿真结果。(a)像旋转器由一面反射镜与一块棱镜组成；(b)像旋转器为 $0°$ 时探测器上的图像；(c)像旋转器为 $22.5°$ 时探测器上的图像；(d)像旋转器为 $45°$ 时探测器上的图像

Fig. 3　Image rotator design scheme and simulation results. (a) Image rotator consists of a mirror and a prism; (b) image on detector at image rotator of $0°$; (c) image on detector at image rotator of $22.5°$; (d) image on detector at image rotator of $45°$

2.3　实验结果

在完成系统搭建与调试后，对系统的性能进行标定。在标定测试过程中，将德国 Nanoscribe 公司生产的 IP-dip 双光子专用光刻胶作为标准光刻胶样品，刻写时将物镜直接浸没到光刻胶中。使用蔡司 Sigma300 扫描电子显微镜（SEM）对样品的表面形貌

进行表征。第一项测试是观察六通道间距的均匀性。本系统实际上是将 AOMC 处的像通过若干透镜成像到物镜的焦平面处。通过分析可知 AOMC 处的像 I_{AOMC} 与物镜焦平面处的像 I_{OBJ} 之间满足 $I_{\text{AOMC}} = 285.7 I_{\text{OBJ}}$。AOMC 每相邻通道之间的间距为 2.5 mm,基于上述公式可以计算得到物镜焦平面处相邻通道之间的间距为 8.75 μm。图 4(a)展示的是实测物镜焦平面处多通道刻写线条的间距,每相邻通道之间的间距为 8.7 μm。测量值与理论值相比误差为 50 nm,该误差在测量误差允许的范围内。可以发现,相较于每一路都独立设计光路来实现多光束刻写,利用 SLM 和 AOMC 配合实现相同的功能不仅可以简化设计,还具有通道间距均匀性高的优势。第二项测试为特征尺寸测量。根据双光子聚合理论,特征尺寸主要由两个因素决定,一是光刻胶,二是激光曝光剂量。本系统使用德国 Nanoscribe 公司的 IP-dip 光刻胶,该光刻胶已被证明可用于 100 nm 级高精度结构的刻写。图 4(b)展示的是转镜在最高旋转频率 32 kHz 条件下的实验结果,其他转速下也能得到类似的结果。图中显示的均是单次扫描得到的刻线。由

图 4(b)可见,随着激光功率从 35 mW 降至 18 mW,线宽从 260.5 nm 降至 74.31 nm,但当线宽小于 150 nm 以后,图形开始从线条变成点阵。这是因为实验中使用的是 80 MHz 的飞秒激光器,在 32 kHz 的旋转频率下,物镜焦平面处的直写速度约为 8 m/s,此时相邻两脉冲之间的间隔约为 100 nm。当线宽较大时,相邻脉冲刻写的点连在一起形成线条,而当线宽下降到 150 nm 以下时,100 nm 间隔无法有效填充,从而形成点阵。因此,本系统的特征尺寸约为 150 nm。使用更高重复频率的激光器或降低转速来减小脉冲间隔,可以获得更小的特征尺寸。第三项测试是标定扫描速度。该项测试将加载一个已知的方波信号到 AOMC 上,在方波信号范围内,AOMC 打开光通道完成刻写。由于方波信号持续时间已知,因此通过测量刻写线条的长度便可以精确计算出扫描速度。为了保证方波信号准确加载,需要将转镜与 AOMC 的开关同步。同步方式是给转镜额外增加一路探测光,该路探测光由一台小型 650 nm 半导体激光器输出,入射到转镜上,反射光不进入扫描透镜,并通过光电探测器进行收集。当转镜开始旋转后,光电探测器获得一个周期性脉冲信号。
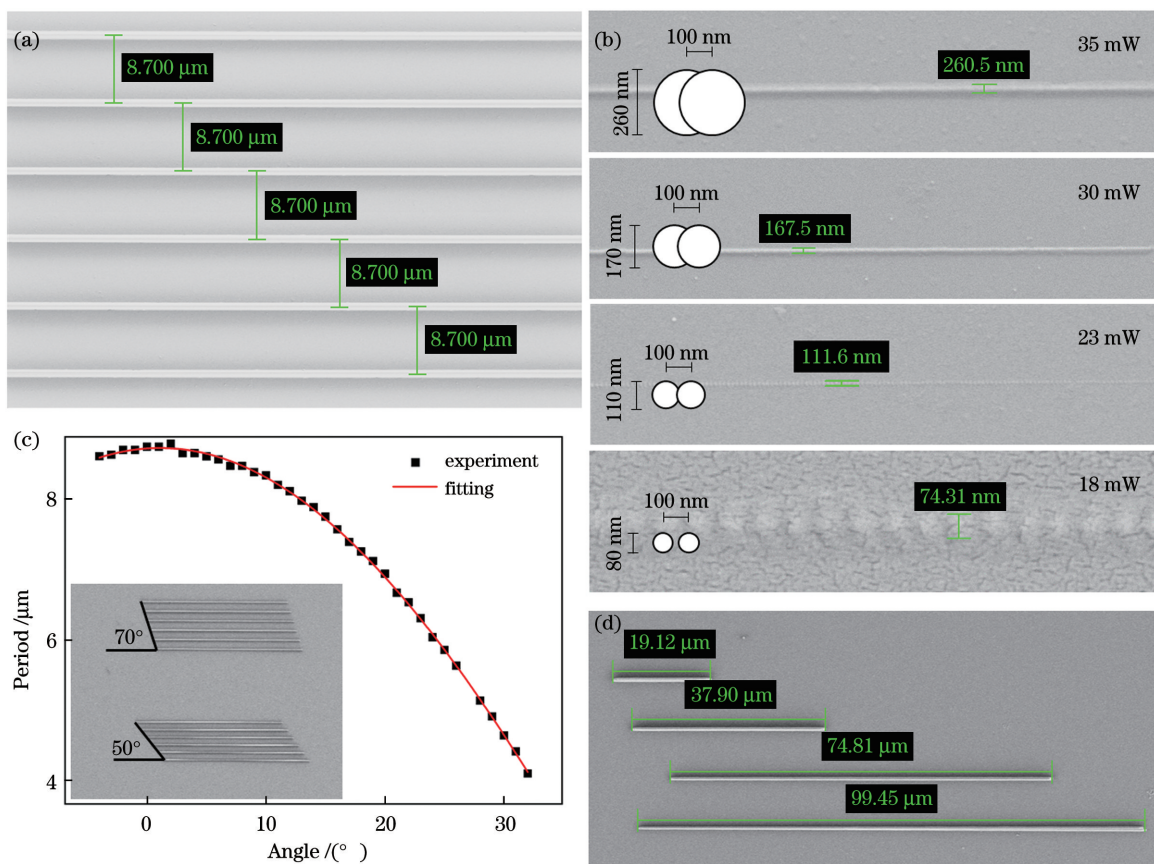

图 4 系统参数标定。(a)六光束间距均匀性;(b)特征尺寸约为 150 nm 线宽低于 150 nm 时线条变成点阵;(c)像旋转器的调节效果,对于精度为 0.02°的旋转台,周期间距调节的精度最高可达 0.3 nm;(d)直写速度标定,从上到下分别对应 1.494、2.961、5.845、7.770 m/s

Fig. 4 System parameters calibration. (a) Six-beam spacing uniformity; (b) feature size is about 150 nm and line changes to lattice when the line-width is below 150 nm; (c) rotator adjustment effect, for a rotary stage with a resolution of 0.02°, the accuracy of period spacing adjustment is up to 0.3 nm; (d) direct writing speed calibration, the speed from top to bottom is 1.494, 2.961, 5.845, 7.770 m/s, respectively

实验中调节所要加载方波与该脉冲信号的时间延迟,就可以连续调节方波信号与转镜扫描起点的时间间隔。图 4(d)展示的是使用时间间隔为 12.8 μs 的方波时测得的刻线,这 4 条刻线从上到下分别对应 6、12、24、32 kHz 的转镜扫描频率。通过计算可以得到 6、12、24、32 kHz 扫描频率下单通道的直写速度分别为 1.494、2.961、5.845、7.770 m/s。该直写速度远高于传统振镜能够达到的直写速度(约为 100 mm/s)。第四项测试是对像旋转器进行标定。通过理论计算可知通道间距 D_{line} 与像旋转器角度 $\varphi_{rotator}$ 之间的关系满足

$$D_{line} = a \cdot \cos k \cdot \pi / [180 \cdot (\varphi_{rotator} - \varphi_0)], \quad (1)$$

式中:φ_0 表示通道间距最大时像旋转器的位置;a 表示最大通道间距;k 表示图像旋转角度与像旋转器旋转角度之间的倍率。本系统中 k 为固定值($k=2$),a 和 φ_0 通过实验确定。在测试过程中,像旋转器被固定到一个中空的电动旋转台上,通过控制旋转台带动像旋转器旋转,从而改变多光束排列方向与转镜扫描方向的夹角。图 4(c)是测试结果,图中黑色方块的横坐标是像旋转器的绝对位置,纵坐标是通过 SEM 测得的通道间距。SEM 插图展示了通道间距被像旋转器调制。利用式(1)对数据进行拟合,可得到 $a = 8.7 \mu m$,$\varphi_0 = 1.1°$。本系统使用的旋转台的精度为 0.02°,根据式(1)可计算得到通道间距的调节精度最高为 0.3 nm。

在完成参数标定后,本团队又进行了打点与小范围编程刻写测试。图 5(a)是打点测试结果。本次测试采用了一种比较巧妙的扫描策略,具体做法如下:首先控制位移台以相对较低的速度运动,随后在每次接收到转镜触发信号后,用一个持续时间极短的方波控制 AOMC 开关,当开关时间足够短时,转镜的扫描轨迹就会由线变成点,从而实现打点效果。在测试过程中,位移台的移动速度为 8000 $\mu m/s$,方波的持续时间为 200 ns,转镜的扫描频率为 6 kHz,即打点速度为 6000 point/s。图 5(b)是小范围编程测试结果,图中每个文字的尺寸约 6 μm×6 μm。在刻写过程中,六通道同步开启,转镜作为 X 轴,位移台作为 Y 轴。在该策略中,每个通道的波形独立生成,实现六通道独立控制。每个通道负责刻写一行文字,当第 1 行文字完成时,第 6 行文字也刻写完成(每行文字不同),大幅提高了刻写效率。
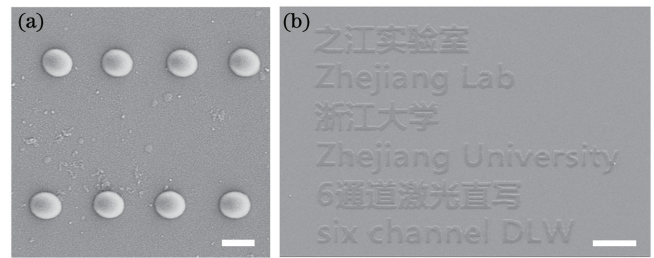

图 5　编程刻写结果。(a)打点测试,比例尺为 500 nm;(b)多通道编程刻写,比例尺为 10 μm

Fig. 5　Programming writing results. (a) Dot writing test, scale bar is 500 nm; (b) multichannel programming writing, scale bar is 10 μm

3　分析与讨论

将本文的实验结果与现有文献结果进行对比,结果如表 1 所示。在扫描速度方面,本系统单通道可以实现近 8 m/s 的刻线速度,在目前的双光子激光直

表 1　近期文献报道的双光子激光直写扫描速度、名义特征尺度以及通道数

Table 1　Two-photo direct writing scanning speed, nominal feature sizes and the number of beams reported in recent literature

Positioning mechanism	Scanning speed /(mm · s^{-1})	Nominal feature size /μm	The number of beams	System index	Ref.
Stepper motor stage	10	1	1	4.0	[31]
Piezo stage	0.09	0.28	1	2.5	[21]
	0.06	0.065	1	3.0	[20]
	30	1.5	1	4.3	[19]
	0.4	10	1	1.6	[18]
	1	1	60	4.8	[13]
Digital micromirror device (DMD)	5	0.5	4	4.6	[32]
Galvo mirror	7	0.78	1	4.0	[26]
	200	0.2	1	6.0	[24]
	103	0.086	1	6.1	[25]
	400	1	1	5.6	[22]
	400	0.5	9	6.9	[1]
	0.1	0.12	9	3.9	[33]
	1	0.1	16	5.2	[16]
Resonant-galvo mirror	8200	1	1	6.9	[27]
This work	7770	0.15	6		8.4

写工作中,只有共振振镜的直写速度与本系统处在同一数量级。但在特征尺寸方面,本系统在 150 nm 级别,而共振振镜方案则在 1 μm 左右。为了更全面地比较不同系统直写速度的差别,这里定义了一个新的参量,本文将其命名为系统指数(system index)S_I。S_I 的定义为

$$S_I = \lg_{10}\left(v_{scan} \cdot \frac{n}{d_{feature}}\right), \quad (2)$$

式中:v_{scan} 表示单通道直写速度;n 表示通道数;$d_{feature}$ 表示特征尺寸。从式(2)中可以看到:光束数量越多,直写速度越快;特征尺寸越小,系统指数越大。表 1 的统计结果表明:本系统在综合刻写效率上具有一定优势。

4 结 论

本团队利用 SLM 产生 6 束光束,使用多通道 AOMC 对每束光的开关与光强进行独立控制。基于转镜与二维位移台实现高速刻写。在 100× 物镜下,单通道直写速度最高达到 7.770 m/s,并行刻写时直写速度可达 46.62 m/s。刻写特征尺寸为 150 nm。这些结果初步验证了该系统在高速刻写方面的潜力。通过对比现有文献可知本系统在刻写效率方面具有较大优势。此外,本系统中多光束数量的限制在于多通道 AOMC 器件以及激光能量,更换具有更多通道的 AOMC 和更高功率的激光源可以比较容易地实现光束数量的增加,从而进一步提高刻写效率。本系统在刻写策略方面仍有很大提升空间,后续将继续研究刻写策略对刻写效率的影响。此外,本系统可结合边缘抑制技术进一步提高分辨率[34]。本工作在提高双光子激光直写技术的直写速度方面具有重要意义,有助于该项技术向产业化应用推进。

参 考 文 献

[1] Hahn V, Kiefer P, Frenzel T, et al. Rapid assembly of small materials building blocks (voxels) into large functional 3D metamaterials[J]. Advanced Functional Materials, 2020, 30(26): 1907795.

[2] Malinauskas M, Žukauskas A, Hasegawa S, et al. Ultrafast laser processing of materials: from science to industry[J]. Light: Science & Applications, 2016, 5(8): e16133.

[3] Lin W, Chen D H, Chen S. Emerging micro-additive manufacturing technologies enabled by novel optical methods[J]. Photonics Research, 2020, 8: 1827-1842.

[4] Frenzel T, Kadic M, Wegener M. Three-dimensional mechanical metamaterials with a twist[J]. Science, 2017, 358(6366): 1072-1074.

[5] Aristov A I, Manousidaki M, Danilov A, et al. 3D plasmonic crystal metamaterials for ultra-sensitive biosensing[J]. Scientific Reports, 2016, 6: 25380.

[6] Maigyte L, Purlys V, Trull J, et al. Flat lensing in the visible frequency range by woodpile photonic crystals[J]. Optics Letters, 2013, 38(14): 2376-2378.

[7] Wu D, Wu S Z, Xu J, et al. Hybrid femtosecond laser microfabrication to achieve true 3D glass/polymer composite biochips with multiscale features and high performance: the concept of ship-in-a-bottle biochip[J]. Laser & Photonics Reviews, 2014, 8(3): 458-467.

[8] Liberale C, Cojoc G, Bragheri F, et al. Integrated microfluidic device for single-cell trapping and spectroscopy[J]. Scientific Reports, 2013, 3: 1258.

[9] Gissibl T, Thiele S, Herkommer A, et al. Two-photon direct laser writing of ultracompact multi-lens objectives[J]. Nature Photonics, 2016, 10(8): 554-560.

[10] Dietrich P I, Blaicher M, Reuter I, et al. In situ 3D nanoprinting of free-form coupling elements for hybrid photonic integration[J]. Nature Photonics, 2018, 12(4): 241-247.

[11] Mačiulaitis J, Deveikytė M, Rekštytė S, et al. Preclinical study of SZ2080 material 3D microstructured scaffolds for cartilage tissue engineering made by femtosecond direct laser writing lithography[J]. Biofabrication, 2015, 7(1): 015015.

[12] Richter B, Hahn V, Bertels S, et al. Guiding cell attachment in 3D microscaffolds selectively functionalized with two distinct adhesion proteins[J]. Advanced Materials, 2017, 29(5): 1604342.

[13] Yang L, El-Tamer A, Hinze U, et al. Parallel direct laser writing of micro-optical and photonic structures using spatial light modulator[J]. Optics and Lasers in Engineering, 2015, 70: 26-32.

[14] Yan W S, Cumming B P, Gu M. High-throughput fabrication of micrometer-sized compound parabolic mirror arrays by using parallel laser direct-write processing[J]. Journal of Optics, 2015, 17(7): 075803.

[15] Vizsnyiczai G, Kelemen L, Ormos P. Holographic multi-focus 3D two-photon polymerization with real-time calculated holograms[J]. Optics Express, 2014, 22(20): 24217-24223.

[16] Gittard S D, Nguyen A, Obata K, et al. Fabrication of microscale medical devices by two-photon polymerization with multiple foci via a spatial light modulator[J]. Biomedical Optics Express, 2011, 2(11): 3167-3178.

[17] Obata K, Koch J, Hinze U, et al. Multi-focus two-photon polymerization technique based on individually controlled phase modulation[J]. Optics Express, 2010, 18(16): 17193-17200.

[18] Chu W, Tan Y X, Wang P, et al. Centimeter-height 3D printing with femtosecond laser two-photon polymerization[J]. Advanced Materials Technologies, 2018, 3(5): 1700396.

[19] Ovsianikov A, Deiwick A, van Vlierberghe S, et al. Laser fabrication of three-dimensional CAD scaffolds from photosensitive gelatin for applications in tissue engineering[J]. Biomacromolecules, 2011, 12(4): 851-858.

[20] Haske W, Chen V W, Hales J M, et al. 65 nm feature sizes using visible wavelength 3-D multiphoton lithography[J]. Optics Express, 2007, 15(6): 3426-3436.

[21] Straub M, Gu M. Near-infrared photonic crystals with higher-order bandgaps generated by two-photon photopolymerization[J]. Optics Letters, 2002, 27(20): 1824-1826.

[22] Skylar-Scott M A, Liu M C, Wu Y L, et al. Guided homing of cells in multi-photon microfabricated bioscaffolds[J]. Advanced Healthcare Materials, 2016, 5(10): 1233-1243.

[23] Bückmann T, Thiel M, Kadic M, et al. An elasto-mechanical unfeelability cloak made of pentamode metamaterials[J]. Nature Communications, 2014, 5: 4130.

[24] Obata K, El-Tamer A, Koch L, et al. High-aspect 3D two-photon polymerization structuring with widened objective working range (WOW-2PP)[J]. Light: Science & Applications, 2013, 2(12): e116.

[25] Gottmann J. High speed and high precision fs-laser writing using a scanner with large numerical aperture[J]. Journal of Laser Micro, 2009, 4(3): 192-196.

[26] Farsari M, Filippidis G, Sambani K, et al. Two-photon polymerization of an eosin Y-sensitized acrylate composite[J]. Journal of Photochemistry and Photobiology A: Chemistry, 2006, 181(1): 132-135.

[27] Pearre B W, Michas C, Tsang J M, et al. Fast micron-scale 3D

printing with a resonant-scanning two-photon microscope[J]. Additive Manufacturing, 2019, 30: 100887.

[28] di Leonardo R, Ianni F, Ruocco G. Computer generation of optimal holograms for optical trap arrays[J]. Optics Express, 2007, 15(4): 1913-1922.

[29] Lin H, Jia B H, Gu M. Dynamic generation of Debye diffraction-limited multifocal arrays for direct laser printing nanofabrication[J]. Optics Letters, 2011, 36(3): 406-408.

[30] Kim D U, Song H, Song W, et al. Two-photon microscopy using an Yb^{3+}-doped fiber laser with variable pulse widths[J]. Optics Express, 2012, 20(11): 12341-12349.

[31] Kumi G, Yanez C O, Belfield K D, et al. High-speed multiphoton absorption polymerization: fabrication of microfluidic channels with arbitrary cross-sections and high

aspect ratios[J]. Lab on a Chip, 2010, 10(8): 1057-1060.

[32] Geng Q, Wang D E, Chen P F, et al. Ultrafast multi-focus 3-D nano-fabrication based on two-photon polymerization[J]. Nature Communications, 2019, 10: 2179.

[33] Dong X Z, Zhao Z S, Duan X M. Micronanofabrication of assembled three-dimensional microstructures by designable multiple beams multiphoton processing[J]. Applied Physics Letters, 2007, 91(12): 124103.

[34] 周国尊, 何敏菲, 杨臻垚, 等. 基于边缘光抑制技术的双光束激光直写纳米光刻系统[J]. 中国激光, 2022, 49(2): 0202001.
Zhou G Z, He M F, Yang Z Y, et al. Dual-beam laser direct writing nano-lithography system based on peripheral photoinhibition technology[J]. Chinese Journal of Lasers, 2022, 49(2): 0202001.

High-Speed Parallel Two-Photon Laser Direct Writing Lithography System

Wang Hongqing[1], Wen Jisen[1], Yang Zhenyao[1], Tang Mengbo[1], Sun Qiuyuan[1],
Ma Chengpeng[1], Wang Ziang[2], Zhan Lanxin[1], Zhang Xiaoyi[1], Cao Chun[1], Shen Xiaoming[1],
Ding Chenliang[1*], Kuang Cuifang[1,2**]

[1] *Research Center for Intelligent Chips and Devices, Zhejiang Laboratory, Hangzhou 310023, Zhejiang, China*;

[2] *State Key Laboratory of Modern Optical Instrumentation, College of Optical Science and Engineering, Zhejiang University, Hangzhou 310027, Zhejiang, China*

Abstract

Objective Recently, two-photon three-dimensional laser direct writing technology has realized fast development and gradually developed into a mature micro/nanofabrication technology. However, this technology is currently largely employed in laboratories. A limitation is the low direct writing speed. A simple and efficient approach to enhance the direct writing speed is to employ multibeam parallel writing instead of single beam writing. Some research has already employed a spatial light modulator or a diffractive optical element to produce multibeam parallel writing. However, till now, multibeam direct writing cannot be separately modulated for each channel, or the modulation speed is too slow, which has been unable to achieve a high-speed direct writing scheme with industrial application value. In addition, employing various motion scanning devices is also an effective means to improve the direct writing speed. In the previous work, piezoelectric stage is usually used for motion control. However, it can only attain a scanning speed of 0.1–10 mm/s. A faster, conventional solution is to employ a galvanometer, which can increase the speed by 1–2 orders of magnitude because of its low inertia. Recently, a study group employed the resonant galvanometer to achieve a higher scanning speed, up to 8 m/s, but the precision was low and the feature size was 1–4 μm. In this study, we design and verify a six-channel high-speed two-photon laser direct writing system, with a maximum direct writing speed of 7.770 m/s per channel, a feature size of 150 nm, and a comprehensive direct writing speed of 46.62 m/s in parallel writing.

Methods In this research, we employ a 780 nm femtosecond laser as the light source and precompensate the group velocity dispersion using a grating pair module. The laser beam was modulated using a spacial light modulator to produce multiple beams. A weighted Gerchberg-Saxton algorithm is employed to create a six-beam hologram and produce a multibeam with high uniformity through continuous iteration. The multibeam is focused on a multichannel acoustic optical modulator (AOMC), to achieve high-speed independent modulation of the multibeam. Then the spot is imaged to a polygon laser scanner's plane, which is employed to conduct the X-axis scan, and the 3D scanning is achieved using a linear stage with air bearings as Y-axis and a piezoelectric stage as Z-axis. Furthermore, a reflective image rotator is designed in this study (Fig. 3), which is positioned before the polygon laser scanner to adjust channel spacing continuously.

Results and Discussions In this study, IP-dip two-photon photoresist made by Nanoscribe in Germany is employed as the standard photoresist sample. The first test was channel spacing uniformity. The distance between each adjacent channel is 8.7 μm [Fig. 4(a)], which is extremely close to the computed value of 8.75 μm. Compared with independently designing optical paths for each beam in the multibeam writing, employing SLM and AOMC to achieve the same function cannot only simplify the design but also has the benefit of high uniformity in channel spacing. The feature

size measurement is the second test [Fig. 4(b)]. At the highest direct writing speed (~8 m/s), the line width decreases from 260.5 nm to 74.31 nm as the laser power decreases from 35 mW to 18 mW; however, after 150 nm, the lines start to form a lattice. The feature size of this system is approximately 150 nm, although a smaller feature size can be achieved by switching to a laser with a higher repetition frequency or employing low-speed direct writing. The third test was scanning speed [Fig. 4(d)]. In the single-channel mode, our maximum direct writing speed is 7.770 m/s and more than 46 m/s in six channels. The fourth test is to calibrate the image rotator [Fig. 4(c)]. The rotating stage's precision employed in this system is 0.02°, according to equation (1), the adjustment accuracy of channel spacing is up to 0.3 nm. Additionally, this research performed the dot [Fig. 5(a)] and a programming test [Fig. 5(b)]. Table 1 compares the most recent literature studies on two-photon laser direct writing. In terms of scanning speed, our system obtains a speed of about 8 m/s at the single-channel mode, and in terms of feature size, our system reaches 150 nm, which is better than most studies.

Conclusions　　In this study, SLM is employed to create six beams, and AOMC is employed to separately control the switching and intensity of each beam. High-speed writing is achieved based on a polygon laser scanner and two-dimensional linear stage with air bearings. The direct writing speed is 7.770 m/s in single-channel mode, and over 46 m/s at parallel writing. The feature size is approximately 150 nm. The system's potential in high-speed writing was preliminarily confirmed. Furthermore, this system's AOMC devices and laser energy serve as a limitation on the number of beams it can produce. It is easy to increase the number of beams by replacing more channel AOMC and higher power laser sources, therefore enhancing the writing's effectiveness. However, there is still room for enhancement in the system's writing strategy, which will be further investigated in the future. This study is of significant benefit in enhancing the writing speed of two-photon laser direct writing technology, which is helpful for the technology to advance toward greater industrial use.

Key words　　optical fabrication; micro- and nanofabrication; two-photon laser direct writing; parallel fabrication of multiple beams